forests

MDPI

Article

Spatial Variability of Soil CO_2 Emissions and Microbial Communities in a Mediterranean Holm Oak Forest

Claudia Di Bene [1,*], Loredana Canfora [1], Melania Migliore [1,2], Rosa Francaviglia [1] and Roberta Farina [1]

[1] Council for Agricultural Research and Economics, Research Centre for Agriculture and Environment, Via della Navicella 2–4, 00184 Rome, Italy; loredana.canfora@crea.gov.it (L.C.); melania.migliore@crea.gov.it (M.M.); r.francaviglia@gmail.com (R.F.); roberta.farina@crea.gov.it (R.F.)
[2] PlantLab, Center of Plant Sciences, Scuola Superiore Sant'Anna, Piazza Martiri della Libertà 33, 56127 Pisa, Italy
* Correspondence: claudia.dibene@crea.gov.it

Abstract: Forests play a key role in the global carbon (C) cycle through multiple interactions between above-ground and soil microbial communities. Deeper insights into the soil microbial composition and diversity at different spatial scales and soil depths are of paramount importance. We hypothesized that in a homogeneous above-ground tree cover, the heterogeneous distribution of soil microbial functional diversity and processes at the small scale is correlated with the soil's chemical properties. From this perspective, in a typical Mediterranean holm oak (*Quercus ilex* L.) peri-urban forest, soil carbon dioxide (CO_2) emissions were measured with soil chambers in three different plots. In each plot, to test the linkage between above-ground and below-ground communities, soil was randomly sampled along six vertical transects (0–100 cm) to investigate soil physico-chemical parameters; microbial processes, measured using Barometric Process Separation (BaPS); and structural and functional diversity, assessed using T-RFLP and qPCR Real Time analyses. The results highlighted that the high spatial variability of CO_2 emissions—confirmed by the BaPS analysis—was associated with the microbial communities' abundance (dominated by bacteria) and structural diversity (decreasing with soil depth), measured by H' index. Bacteria showed higher variability than fungi and archaea at all depths examined. Such an insight showed the clear ecological and environmental implications of soil in the overall sustainability of the peri-urban forest system.

Keywords: barometric process separation; functional diversity; multivariate analysis; soil CO_2 emissions; soil microorganisms; spatial distribution; T-RFLP

Citation: Di Bene, C.; Canfora, L.; Migliore, M.; Francaviglia, R.; Farina, R. Spatial Variability of Soil CO_2 Emissions and Microbial Communities in a Mediterranean Holm Oak Forest. *Forests* **2024**, *15*, 2018. https://doi.org/10.3390/f15112018

Academic Editors: Shengqiang Wang, Yili Guo, Qiqian Wu and Pujia Yu

Received: 3 September 2024
Revised: 29 October 2024
Accepted: 1 November 2024
Published: 15 November 2024

1. Introduction

The Mediterranean Basin is considered a primary hotspot for climate change, since droughts and heatwaves are causing less rainfall with hotter and drier summers in comparison with other regions of the world [1]. In this context, Mediterranean forests represent one of the most endangered ecosystems worldwide due to the detrimental effects of climate change [2]. Understanding the need for adaptation and mitigation of the Mediterranean forests in the context of global environmental change is critical for developing appropriate sustainable management strategies and policy plans. Thus, new high-level forest-related strategies such as Sustainable Development Goal number 15 of the 2030 Agenda for Sustainable Development of the United Nations adopted in 2015, the new EU Strategy for Biodiversity, and the new EU Forest Strategy for 2030 have been approved both at the global and EU level to protect, restore, and promote the sustainable management of forests and halt biodiversity loss [3].

In this context, soils of the Mediterranean forests are of crucial importance in climate processes [4,5] and the global carbon (C) cycle [6] because they represent a hotspot for biodiversity and are directly involved in climate change mitigation and adaptation management strategies by regulating soil–atmosphere greenhouse gas (GHG) emissions [7].

The spatio-temporal variation in GHG emissions is mainly affected by soil microbial processes [8] such as nitrification, denitrification, and respiration. In particular, soil microbial respiration is considered the primary natural source for carbon dioxide (CO_2) emissions, exceeding any other terrestrial–atmosphere C transactions [9].

The accurate assessment of this flux is challenging because the C pool is influenced by many factors such as land cover (vegetation species), meteorological factors (i.e., temperature and rainfall), soil properties (i.e., soil texture, microbial communities, pH, and C/N ratio), and anthropogenic activities [10,11].

In forest ecosystems, soil microbial processes greatly affect the gas exchanges in the soil–plant continuum [12]. Microbial communities are sensitive to climate variations and disturbances at a microscopic scale [13]; however, high diversity helps to reduce the fluctuations of soil processes, demonstrating that biodiversity becomes important under changing environmental conditions [14]. Thus, microbial structure, diversity, and functions could explain the spatial heterogeneity in ecosystem processes [15,16]. Nevertheless, few studies have linked microbial diversity and processes to assess the magnitude and stability of GHG emissions in forest soils [17]. Therefore, investigations of the soil microbial communities' abundance and structure (e.g., fungi to bacteria ratio) in forest ecosystems are needed to understand the contribution of these communities to the soil–atmosphere C exchange, in the climate change mitigation strategies challenge [18]. So far, key uncertainties remain about the microbial spatial variability along a soil depth gradient and the influence of the microbial community in regulating the C biogeochemical cycle. Thus, in this study we aimed to understand how the most reliable and sensitive soil physico-chemical properties and soil microbial community diversity—at different spatial levels and along a soil depth gradient—influence soil CO_2 emissions of a Mediterranean peri-urban holm oak (*Quercus ilex* L.) coverage forest.

For this reason, we addressed the following topical questions: (1) How does spatial variability influence soil CO_2 emissions? (2) How do soil properties regulate these changes and the soil C biogeochemical cycle? (3) How do soil organic carbon (SOC) and microbial community diversity vary with the spatial scale and along a 100 cm soil depth gradient?

Based on these knowledge needs, we used a multi-parameter approach to investigate (i) the spatial heterogeneity of CO_2 emissions, measured at soil level using a portable dynamic respiration chamber; (ii) biogeochemical processes, simultaneously measuring nitrification, denitrification, and microbial respiration rates using the Barometric Process Separation (BaPS) method; and (iii) the spatial distribution of the below-ground microbiological community using Terminal-Restriction Fragment Polymorphism (T-RFLP) and qPCR Real Time analyses.

2. Materials and Methods

2.1. Study Area

This study was conducted in a typical Mediterranean peri-urban holm oak forest (*Quercus ilex* L.) located within the Presidential Estate of Castelporziano (c.a. 6000 ha), a natural reserve since 1970, 25 km SW from Rome city center, Italy (41°70′42″ N, 12°35′72″ E; altitude 13 m a.s.l.). The forest is an unmanaged rear dune ecosystem 1.5 km from the Tyrrhenian seashore. The canopy height is homogeneous (14 m), with a leaf area index of 3.69 m^2 leaf m^{-2} ground; small shrubs of *Phillyrea latifolia* are poorly distributed beneath the main canopy. The soil, with flat topography, sandy texture, low water-holding capacity, and being well-drained, is classified as *Typic Xeropsamment* following the USDA system [19] and as *Haplic Luvisols* following the FAO [20].

The main physical and chemical properties of the 0–30 cm soil depth are as follows: 851 g kg^{-1} sand (2000–50 µm), 116 g kg^{-1} silt (50–2 µm), and 33 g kg^{-1} clay (<2 µm); pH (H_2O, 1:2.5) 6.9; soil organic C 8.7 g kg^{-1}; soil total N, 0.6 g kg^{-1}; and C/N ratio 13.7. The climate is typically meso-Mediterranean with warm and dry summers, mild winters, and with rainfall mainly concentrated in autumn and spring. The mean annual rainfall and temperature are 728 mm and 16 °C, respectively. The coldest month is January, with a

mean temperature of 6 °C, and the hottest month is August, with a mean temperature of 24 °C. The wind regime is characterized by winds from the sea (S-SW) blowing during the morning, and winds from inland (N-NE) in the afternoon.

At the soil level, capacity relative temperature and humidity sensors (CS 650, Campbell Scientific) were installed at 10, 50, and 100 cm soil depth. All sensors recorded each minute, and data were averaged for 30 min intervals using a datalogger (CR3000, Campbell Scientific, Shepshed, UK).

Additional information and details on the study area are reported in [21–23].

2.2. Experimental Design and Soil CO_2 Emissions Measurement

Between June and November 2013, three plots were set-up within the footprint of the eddy covariance (EC) station (total area of 1080 m^2) to assess spatial variability of soil CO_2 emissions. In each plot, three replicates (n = 3; plots of 360 m^2) were selected in a completely randomized design. One week prior to the soil CO_2 emissions measurement, open-ended PVC collars (10 cm diameter; 5.0 cm height) were permanently inserted 2 cm into the forest floor to limit root severing (three collars per plot, n = 12), reduce CO_2 leaking, and provide a stable seal between chamber and soil surface [24–26]. Collars were placed maintaining a minimal distance of 3 m from any tree. Before each sampling, we removed the litter fallen inside the collars to measure CO_2 emissions only from soil (roots plus microorganisms). Soil CO_2 emissions were measured in the field using the EGM-4 system (EGM-4, Environmental Gas Monitor IRGA system; PP-Systems, Hitchin, Hertfordshire, UK) connected to a soil portable non-steady-state through-flow cylindrical chamber (SRC-1, PP-systems, Hitchin, UK; diameter 10 cm, base area of 78 cm^2, volume 1171 cm^3 changed to 1411 cm^3, considering the inclusion of the collar sticking of 3 cm above the soil surface). At each soil CO_2 emissions measurement, soil temperature was also recorded next to each collar using a probe (STP-1 attached to the EGM-4 system) inserted 5–10 cm into the Soil For more details on the soil chamber device, see [24,27,28]. Soil CO_2 emissions were measured weekly in June, July, September, October, and November 2013. Measurements were always taken between 10 and 14 h, because the midday CO_2 emission values avoid diurnal fluctuations and are assumed to be a better representation of the actual site mean flux [24,25,29]. Soil CO_2 emission rates (μmol CO_2 m^{-2} s^{-1}) were calculated as a linear CO_2 increase regression ($R^2 > 0.95$) using the automatically logged CO_2 data, according to the following equation (Equation (1)):

$$FCO_2 = \frac{PV}{ART} \cdot \frac{dCO_2}{dt} \quad (1)$$

where FCO_2 is soil CO_2 emissions (μmol m^{-2} s^{-1}); P is the atmospheric pressure (kPa); V is the total volume of the headspace gas within the chamber and sampling collar, calculated as the sum of the chamber volume and the collar volume (V = Vchamber + Vcollar; m^3); A is the area of soil enclosed by the chamber (m^2); R is the gas constant; T is the air temperature (°K); and dCO_2/dt is the rate of change of CO_2 concentration (μmol mol^{-1} dry air) in the chamber headspace between two CO_2 measurement points.

2.3. Soil Sampling for Chemical Properties and Microbial Abundance, Diversity, and Processes

In September 2013, in the three plots, soil was sampled to assess chemical properties, microbiological abundance and diversity, and microbial processes. Per each plot, three undisturbed and representative soil samples were obtained by mixing three homogenized soil cores [30] collected in the vertices of a 1 m side equilateral triangle, were sampled using a hand probe coring tube sampler (5 cm inside diameter) according to the procedure in [31,32]. For monitoring chemical properties and microbiological abundance and diversity, soil was sampled from the soil surface down to 100 cm in depth, along with six vertical transects (0–10, 10–20, 20–40, 40–60, 60–80, and 80–100 cm), whilst for monitoring microbial processes, soil cores were sampled with stainless steel cylinder in the 0–20 cm layer [33].

2.4. Soil Chemical Analysis

For chemical analyses, after removing easily detectable litter, residues, and coarse roots, soil samples from all depth intervals were air dried to constant weight and manually passed through a 2 mm sieve [34]. Soil pH was measured in deionized water (1:2.5 soil/water suspension) using a Crison GLP22 pHmeter [35]. Total nitrogen (TN) and soil organic carbon (SOC) concentrations were evaluated using the automated combustion method, using Nitrogen/protein FP628-LECO and Carbon RC612-LECO elemental analyzer, respectively (LECO Corporation, St. Joseph, MI, USA). Soil C/N ratio was calculated as the quotient of SOC and TN concentrations.

2.5. Assessment of Microbial Processes

Barometric Process Separation (BaPS) instrument (UMS GmbH Gmunder Str. 37 D-81379 München, Germany) assessed microbial processes represented by soil respiration (*Rs*, mg C kg^{-1} h^{-1}), denitrification (*Denitr*, mg N kg^{-1} h^{-1}), and gross nitrification (*Nitr*, mg N kg^{-1} h^{-1}) rates in soil samples. Undisturbed soil samples were air dried prior to the analysis and then wetted to field capacity, equilibrated for 72 h at 25 °C, and incubated in the BaPS chamber at 25 °C for 24 h [36–39]. The chamber was immersed in a thermostatic bath to guarantee the thermal equilibrium during the time of analysis. After incubation, the BaPS software (UMS, Version 2.2.4) simultaneously calculated the rates of *Rs*, *Denitr*, and *Nitr* by measuring the changes in gas pressure, O_2, and CO_2 net balances. The change in gas pressure indicates the dominant process occurring: *Rs* is pressure neutral, while *Denitr* and *Nitr* cause a pressure increase and decrease, respectively. The dynamic equilibrium between the CO_2 and O_2 concentrations in headspace and aqueous phase as well as the pH-related solubility is considered in the calculation of the rates of the three processes. More details on BaPS device and measuring processes are given by [9,36–39].

2.6. Microbiological Analytical Procedures

For microbiological abundance and diversity determination, samples were stored at −80 °C and then sieved at field moisture prior to being processed for the analysis.

2.6.1. Extraction of Genomic DNA and PCR Amplification

Genomic DNA was extracted in duplicate from 0.6 g of soil using the PowerSoil DNA Isolation Kit (MoBio Laboratories, Carlsbad, CA, USA) according to the manufacturer's protocol and following the procedures reported in [40]. PCR reactions were repeated three times on each soil sample (technical repeats). PCR reactions were performed in triplicate 50 µL volumes containing 30 ng of DNA, 1.2 µL of each 100 mM primer (forward labeled with the fluorescent dye 5–6 FAM), 10 µL 10× buffer (Promega Corporation, Madison, WI, USA), 1 µL 10 mM dNTP mix, 4 µL 2.5 Mm $MgCl_2$, 1U Taq DNA Polymerase, and PCR-grade water to 50 µL. For the amplification of the bacteria and archaea 16S rRNA gene, the 63f/1087r [41] and Ar3f and Ar927r primers were used, respectively. Reaction conditions were reported in [42]. For the amplification of the fungi ITS and 5.8S rRNA gene regions, the primer ITS1/ITS4 [43] was used. Reaction conditions were as follows: initial denaturation at 95 °C for 5 min, 34 cycles with denaturation at 94 °C for 1 min, annealing at 60 °C for 1 min, extension at 72 °C for 2 min, and a final extension of 8 min at 72 °C. Triplicate PCR reactions were visualized on a 1.5% agarose gel, and then purified with a Qiaquick PCR purification kit (Qiagen, Inc., Chatsworth, CA, USA). Purified products were quantified using Qubit® 2.0 Fluorometer following manufacturer's instructions kit.

2.6.2. Terminal Restriction Fragment Length Polymorphism (T-RFLP)

The digestion of fluorescently labelled PCR fragments using two restriction enzymes was conducted in duplicate as follows: 20 U of TaqI (Promega), 2 µL of 10× buffer, and 300–600 ng of purified PCR product (bacteria and archaea), PCR-grade water to 20 µL, were mixed. The same protocol was followed for AluI (Promega), while for HaeIII and HinfI we used the digestion of fluorescent labelled PCR fungi fragments. The samples

were then incubated for 4 h at 37 °C (TaqI, HaeIII, HinfI) and 65 °C (AluI); the digestion was stopped using incubation at 95 °C for 20 min. Terminal restriction fragment length polymorphism (T-RFLP) products (2 µL) were mixed with 0.3 µL of GeneScanTM 600 LIZ® internal size standard (Applied Byosystems, Darmastadt, Germany) and run on an ABI3500 Genetic Analyzer (Applied Biosystems, Foster city, CA, USA) following the procedures reported in [40]. Diversity indexes were performed using PAST 1.99 software [42]; the analysis was carried out on T-RFLP profiles. Terminal restriction fragment (TRF) numbers, corresponding to OTUs (operational taxonomic units), were calculated, counting numbers of TRFs. The Shannon–Wiener index (also referred to as Shannon Index; *H'*) was used to evaluate the biodiversity [40,41,44].

2.6.3. Quantitative Polymerase Chain Reaction (qPCR)

Quantification of bacteria, archaea, and fungi DNA sequence fragments was carried out using qPCR. Extracted DNA was diluted to 2 ng/µL and stored at −20 °C for the subsequent application. Bacteria DNA was amplified with Muyzer primer pair [45], archaea with Ar364/Ar964 primer pair [46], and fungi with 5.8S/ITS1f primer pair [47]. In brief, all qPCR reactions were carried out in 25 µL reactions with 10 µL of template DNA (2 ng/µL) added to a 20 µL qPCR reaction mixture containing 12.5 µL of QuantiFast Sybr Green PCR Master Mix (Qiagen), 1.2 µM of primer, and PCR-grade water to 15 µL. The reactions were performed in a Stratagene Mx3000P qPCR (Agilent Technologies). Measures were performed in duplicate for each sample. The results were processed using the program provided with the instrument. The absence of primers dimers in amplification products was evaluated analyzing the melting curves of the products considering the fluorescence range 50–99 °C. Standard curves were created from a PCR amplicon for each gene target, considering extract sample of each analyzed plot (depth 0–10 and 10–20 of each spot); the PCR products were purified after the qPCR reaction, then quantified using Qubit® 2.0 Fluorometer following manufacturer's instructions kit and diluted in order to minimize the PCR bias [48]. The gene copy number was calculated using the formula as follows (https://horizondiscovery.com/en/ordering-and-calculation-tools/dna-copy-number-calculation (accessed on 7 November 2024)):

$$\text{Gene copy number} = (\text{ng} \times \text{number/mol})/(\text{base pairs} \times \text{ng/g} \times \text{g mol base pairs}) \quad (2)$$

The standards were created using triplicate 10-fold dilution series covering seven orders of magnitude from 102 to 109 gene copies per qPCR reaction during each run. qPCR reactions were performed in duplicate per DNA and bacteria, archaea, and fungi copy numbers were expressed g^{-1} soil (dry weight).

2.7. Statistical Analysis

For each variable, the normal distribution of the analytical data was checked. Analysis of variance (ANOVA; confidence interval 95%) was performed using XLSTAT version 7.1 software (Addinsoft, Paris, France). One-way ANOVA was used to test the effect of plot on microbial processes at the 20 cm soil depth, while two-way ANOVA was used to test the interactive effect of (i) plot and time of measurement on soil CO_2 emissions, and (ii) plot and soil depth on soil chemical and microbiological data. Data were ln or arcsine transformed when needed to fulfil the assumptions of ANOVA, and Tukey-B procedure was used for comparing means. When data showed neither a normal distribution of error terms nor constant error variance, a non-parametric Kruskal–Wallis test was performed. Means and standard errors given in the tables and graphs are for untransformed data. Multivariate regression analysis (stepwise regression) was used as an exploratory test for investigating the relationship between soil CO_2 emissions and soil temperature and moisture. Linear regressions were used to relate soil chemical and microbiological properties. T-RFLP profiles were converted into presence–absence data and arbitrary classes of soil layers (upper, intermediate, lower) were considered to form three groups. These arbitrary classes were analyzed statistically using cluster analysis based on Bray–Curtis pairwise similarities. Data

on soil chemical properties, soil CO_2 emissions, microbiological processes and diversity were combined as variables in a principal component analysis (PCA), considering the linear response of microbial groups (expressed as absolute abundance of values) to the environmental gradients [49]. The PCA, performed on auto-scaled data, was based on Spearman's rank correlation test that was used both to define the degree of dependence among the variables and to measure the correlation among them.

3. Results

3.1. Soil CO_2 Emissions Measurement with Chambers and Soil Chemical Properties

During the monitoring period (June–November 2013), weather (rainfall and temperature) and soil conditions (temperature and water content at 10 and 100 cm depth) varied considerably, as shown in Figure 1a,b. In detail, rainfall in the June–August months was 8.3-fold lower than that of September–November (Figure 1a). By contrast, the mean air temperature over the 24 h ranged between 11.6 and 27.6 °C (Figure 1a). A period was considered "dry" when the rainfall was equal to or less than twice the mean temperature. As shown in Figure 1b, the soil temperature (°C) ranged between 12.8 and 24.1 °C and from 16.6 to 21.3 °C at soil depths of 10 cm and 100 cm, respectively. The soil moisture (soil water content, SWC; %, *v*:*v*) recorded at 10 cm and 100 cm soil depth ranged from 4.1% to 16.3% and from 6.1% to 31.6%, respectively. The maximum soil moisture values during the soil CO_2 emissions monitoring period occurred in November, while the minimum soil water content was measured in September and coincided with soil temperature values above 19.5 °C. The SWCs logged at 10 cm and 100 cm were negatively correlated with the soil temperature during the whole observation period ($r = -0.543$, $p < 0.001$ and $r = -0.652$, $p < 0.001$; at 10 cm and 100 cm soil depth, respectively). Soil CO_2 emissions were highly variable during the monitoring period, reflecting the seasonal temperature (air and soil) and SWC trend (Figure 1c). The soil CO_2 emissions increased gradually until July, when they reached their peak, which coincided with the seasonal increase in temperature (Figure 1b). Generally, soil CO_2 emissions declined in September and increased with rainfall events in October and November. Although there was a positive response of the soil CO_2 flux to the higher SWC, we found no correlation between soil CO_2 emissions and either SWC or soil temperature over the monitoring period for the three plots. In the measuring period, soil CO_2 emissions ranged between 0.93 and 5.92 μmol CO_2 m^{-2} s^{-1} (10.10 ± 1.48 g CO_2 m^{-2} d^{-1}), between 1.44 and 5.92 μmol CO_2 m^{-2} s^{-1} (1.40 ± 1.47 g CO_2 m^{-2} d^{-1}), and between 1.78 and 8.06 (16.20 ± 2.33 g CO_2 m^{-2} d^{-1}) in plot 1, 2, and 3, respectively. As shown in Figure 1c, the soil CO_2 emissions in plot 3 were significantly higher from June to the end of September compared with the soil CO_2 emissions observed in the other two plots, whereas in October and November an opposite trend was detected. Nevertheless, considering the overall measuring period, in plot 3, the soil CO_2 emissions value was significantly (37%) higher than the value observed in the other two plots.

The soil chemical parameters (mean values ± SE) are reported in Table 1. Considering the three investigated plots and their vertical profile (0–100 cm depth), soil pH values were slightly alkaline, ranging from 7.2 to 7.9, with higher values in the deepest layer (Table 1). Nevertheless, soil pH values were not significantly different among plots and depths ($p = 0.935$). The SOC concentration (g kg^{-1}) was significantly affected by the plot ($p < 0.01$), soil depth ($p < 0.01$), and the plot × soil depth interaction ($p < 0.01$). In the 0–100 cm depth, the highest SOC value ($p < 0.05$) was detected in plot 2 (26.62 g kg^{-1}), followed by plot 3 and plot 1 (20.43 and 17.83 g kg^{-1}, respectively). In detail, the three plots showed similar trends in SOC concentration, with a gradual decrease ($p < 0.05$) from the shallowest (0–10 cm depth) to the deepest layer (80–100 cm depth), with values ranging from 70.62 to 4.20 g kg^{-1} (Table 1). The TN concentration followed a similar trend to SOC, even though there were not statistically significant differences among plots and depths (Table 1). The soil C/N ratio ranged from high (14.30) to low (5.07) values at the 10 cm and 80 cm soil depth, respectively (Table 1). The ratio was significantly different among plots

only in the 0–10 cm and 10–20 cm soil depths, showing an opposite behavior between the first and second layers (P3 different to P1–2, and P1 different from P2–3, respectively).

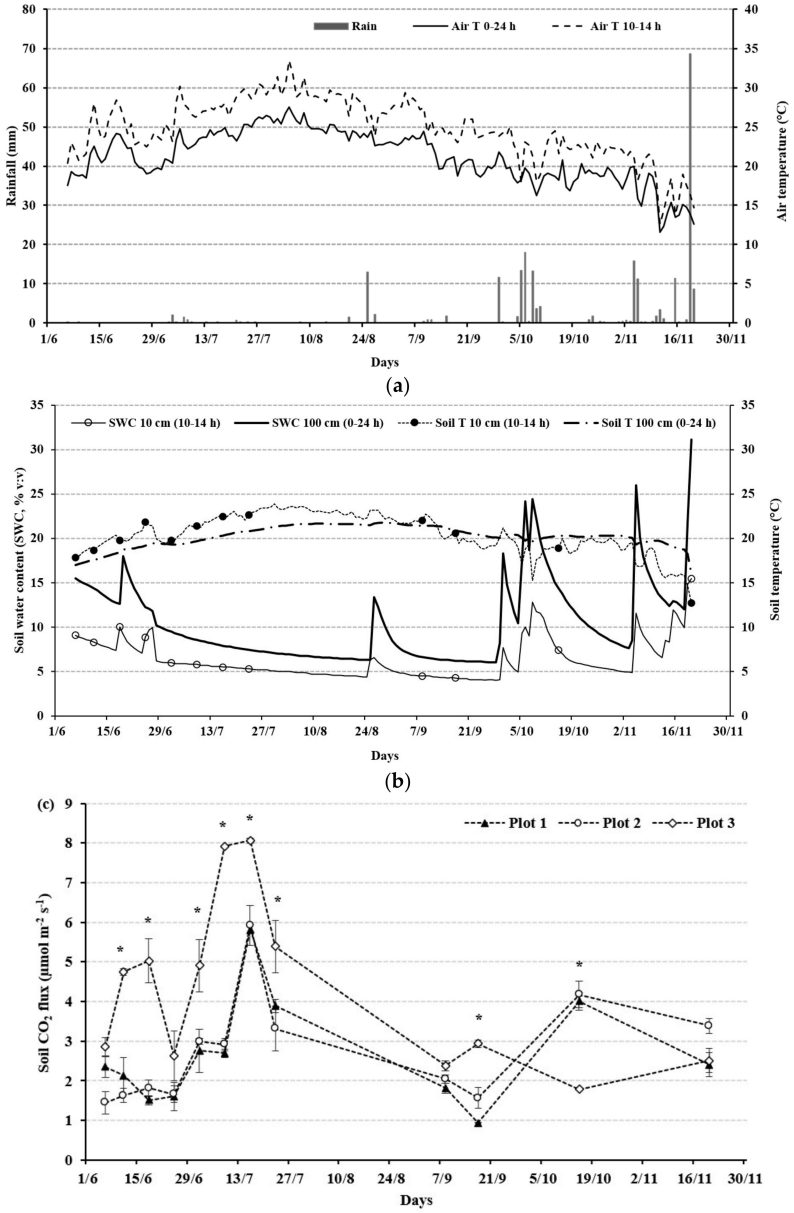

Figure 1. Daily mean air temperature monitored in the 0–24 h (°C) (shown as black continuous line), daily mean air temperature monitored at the time of soil CO_2 emissions measurements between 10 and 14 h (°C) (shown as black dotted line), and daily total rainfall (mm) (shown as gray column) over the soil CO_2 emissions monitoring period at the Castelporziano Reserve (Rome, Italy). A period was considered "dry" when the rainfall was equal to or less than twice the mean temperature (**a**). Daily mean soil temperature (°C) (shown as black dashed line) and daily mean soil water content (%, *v*:*v*) (shown as black continuous line) measured at 10 cm and 100 cm soil depth, respectively, over the soil CO_2 emissions monitoring period. Black and white circles represent daily mean soil temperature and daily mean water content, respectively, monitored at the time of soil CO_2 emissions measurements between 10 and 14 h (°C). (**b**) Soil CO_2 emissions (μmol CO_2 m^{-2} s^{-1}) were measured at the site in three plots (shown as plot 1: black triangle plot 2: white circle and plot 3: white diamond) during the period 6 June to 20 November 2013 with weekly or monthly soil CO_2 emissions monitoring (n = 12). Values are means ± SE (showed as vertical bars) of three replicates for each plot. For each measuring date, statistically significant differences among plots are shown by asterisks according to ANOVA (* $p < 0.05$) (**c**).

Table 1. Depth profile (0–100 cm) of the main soil chemical parameters: pH value (a), soil organic carbon concentration (SOC; g kg^{-1}), total nitrogen concentration (TN; g kg^{-1}), and C/N ratio at the Castelporziano Reserve in the three plots (P1, P2, and P3). Values are means ± SE of three replicates for each plot. For each soil chemical parameter, values not followed by the same small letter and by the same capital letter are significantly different among soil depth within the same plot and among plots within the same soil depth, respectively, according to ANOVA ($p < 0.05$).

Depth	pH			SOC			TN			C/N		
	P1	P2	P3	P1	P2	P3	P1	P2	P3	P1	P2	P3
10	7.15 ± 0.02	7.22 ± 0.01	7.38 ± 0.01	57.19 ± 0.02 aB	83.99 ± 0.02 aA	70.69 ± 0.03 aA	5.02 ± 0.02	7.23 ± 0.04	3.55 ± 0.02	11.40 ± 0.05 B	11.60 ± 0.03 B	19.89 ± 0.02 aA
20	7.19 ± 0.01	7.41 ± 0.01	7.56 ± 0.01	23.93 ± 0.01 bB	37.08 ± 0,01 bA	25.24 ± 0.02 bB	1.29 ± 0.04	3.91 ± 0.04	2.43 ± 0.02	18.53 ± 0.05 A	9.49 ± 0.03 B	10.39 ± 0.02 abB
40	7.22 ± 0.01	7.34 ± 0.01	7.69 ± 0.01	7.09 ± 0.01 cB	19.38 ± 0.02 cA	11.93 ± 0.02 cAB	1.72 ± 0.04	2.34 ± 0.04	2.16 ± 0.02	4.12 ± 0.03	8.29 ± 0.03	5.52 ± 0.03 b
60	7.66 ± 0.01	7.45 ± 0.01	7.72 ± 0.01	14.70 ± 0.02 bcA	11.63 ± 0.02 dA	4.24 ± 0.02 dB	2.07 ± 0.03	2.23 ± 0.01	0.92 ± 0.02	7.09 ± 0.03	5.22 ± 0.02	4.63 ± 0.02 b
80	7.72 ± 0.01	7.89 ± 0.02	7.76 ± 0.02	2.92 ± 0.02 d	3.35 ± 0.02 e	3.31 ± 0.02 d	0.58 ± 0.03	0.63 ± 0.02	0.69 ± 0.02	5.09 ± 0.02	5.29 ± 0.02	4.82 ± 0.02 b
100	7.87 ± 0.01	7.95 ± 0.01	7.80 ± 0.02	1.12 ± 0.02 dB	4.27 ± 0.04 eA	7.20 ± 0.01 cdA	0.14 ± 0.02	0.31 ± 0.01	0.44 ± 0.02	8.65 ± 0.02	13.95 ± 0.01	16.41 ± 0.02 a

3.2. Assessment of Soil Microbial Composition and Processes

Microbial processes (i.e., *Rs*, *Denitr*, and *Nitr*) showed significant differences among all three plots ($p < 0.001$) (Figure 2a–c). *Rs* gradually increased from plot 1 to plot 3 (1.66 ± 0.19 mg C kg^{-1} h^{-1} and 2.45 ± 0.28 mg C kg^{-1} h^{-1}, respectively), with significant differences between plot 1 and 3 (Figure 2a).

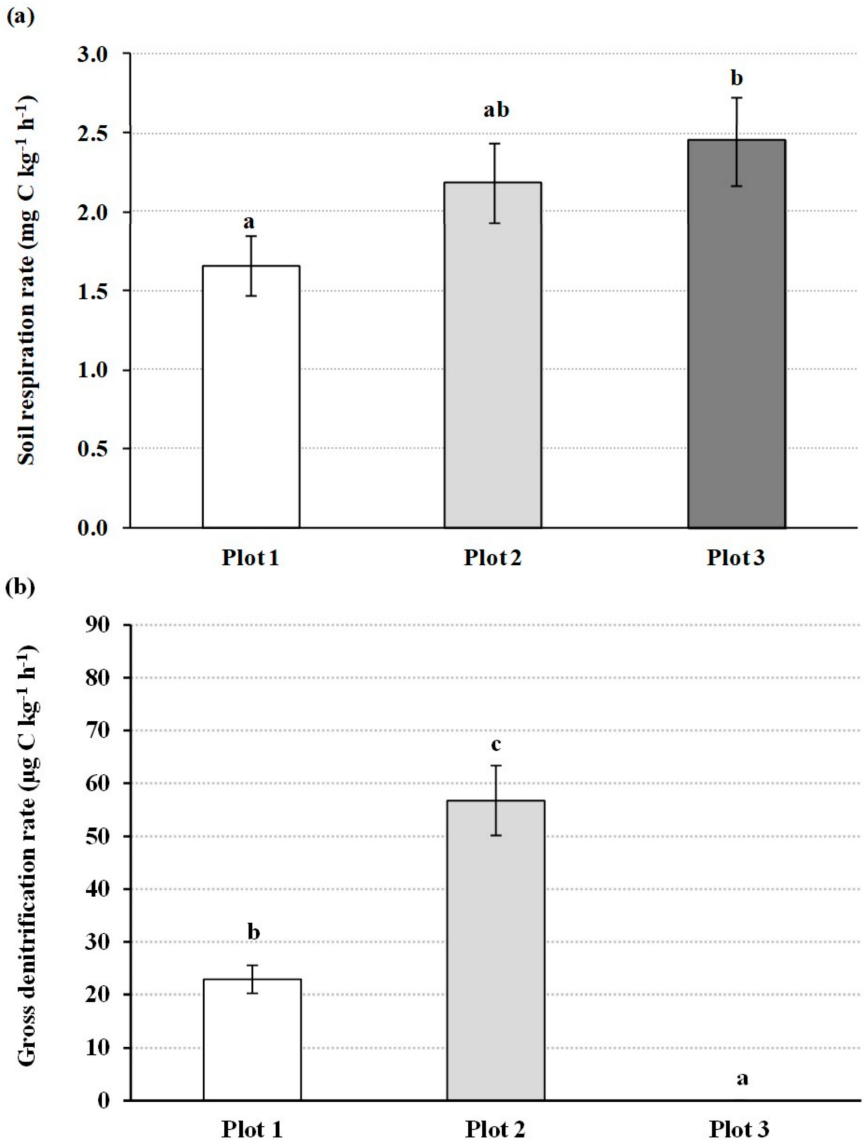

Figure 2. *Cont.*

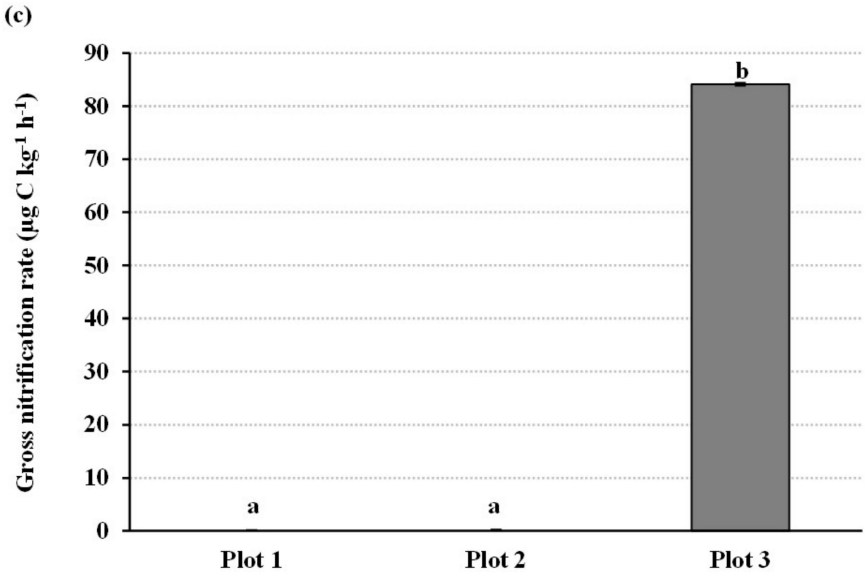

Figure 2. BaPS parameters measured at 0–20 cm layer: soil respiration rate (*RS*; mg C kg^{-1} h^{-1}) (**a**), gross denitrification rate (*Denitr*; µg N kg^{-1} h^{-1}) (**b**), and gross nitrification rate (*Nitr*; µg N kg^{-1} h^{-1}) (**c**). Values are means ± SE (showed as vertical bars) of three replicates for each plot. *Denitr* rate was detected in plots 1–2, while *Nitr* rate was only detected in plot 3. Values not followed by the same small letter are significantly different among plots within the same soil depth, according to ANOVA ($p < 0.05$).

Denitr was detected in plot 1 and 2 (56.75 ± 6.55 µg N kg^{-1} h^{-1} vs. 22.92 ± 2.65 µg N kg^{-1} h^{-1}, respectively; $p < 0.001$) (Figure 2b). *Nitr* was detected only in plot 3 with a gross nitrification rate of 84.13 ± 9.71 µg N kg^{-1} h^{-1} (Figure 2c).

The microbial community abundance showed a similar behavior in all plots. The highest values were observed in the upper layers (10 cm and 20 cm depth), decreasing gradually along the soil profile. In each plot, the abundance was dominated by bacteria, accounting for 93 to 97% of the total, followed by fungi and archaea, which represented 0.39 to 6.77% and 0.01 to 0.04%, respectively (Figure 3). For the bacteria, two significantly different abundance groups could be discriminated between plots 1–2 and plot 3 (Figure 3). Along the soil depth profile, the bacteria abundance was 15% higher in plots 1–2 than in plot 3. Conversely, the archaea abundance was 67% lower in plots 1–2 than in plot 3 (Figure 3). With regard to fungi abundance, in plot 1 it was three orders of magnitude lower in the deepest soil layer (100 cm; 4.52×10^{9}) than in the shallow layer (10 cm; 1.53×10^{12}) in comparison with the other two plots (Figure 3).

3.3. Soil Microbial Structure and Diversity Along the Depth Gradient

The T-RFLP analysis revealed a different microbial community composition among the plots and along the soil depth profile (significant mean differences at $p = 0.0001$; Figure 4). In detail, for the bacteria, a total of 522, 416, and 479 T-RFs was observed in plot 1, 2, and 3, respectively. For archaea, the highest value of T-RFs (a total of 441) was found in plot 2, followed by plot 3 and plot 1, with a total of 436 and 321 T-RFs, respectively. For the fungi, a total of 121, 127, and 114 T-RFs was observed in plot 1, 2, and 3, respectively.

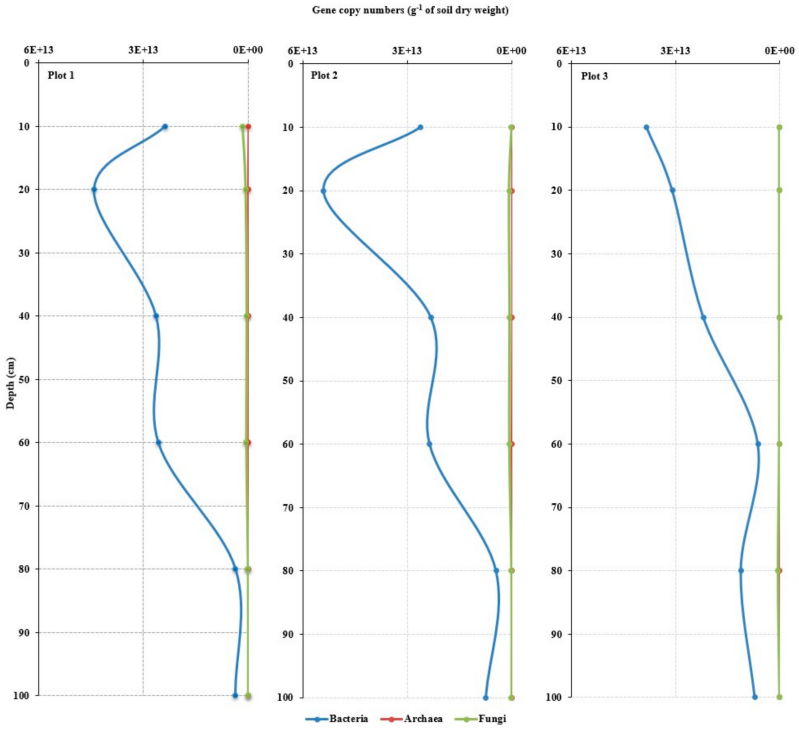

Figure 3. Abundance of bacteria, archaea, and fungi expressed as gene copy numbers (g^{-1} of soil dry weight) as detected along the investigated soil depth profile (0–100 cm) in each plot (bacteria as blue line and dots, archaea as red line and dots, and fungi as green line and dots). The abundance of each microbial community represents the average value of duplicate quantifications using 16S rDNA q-PCR analysis. Gene copy numbers were expressed in scientific notation. 0E+00 and 6E+13 refer to numbers ranging from 5.83×10^8 to 5.40×10^{13}.

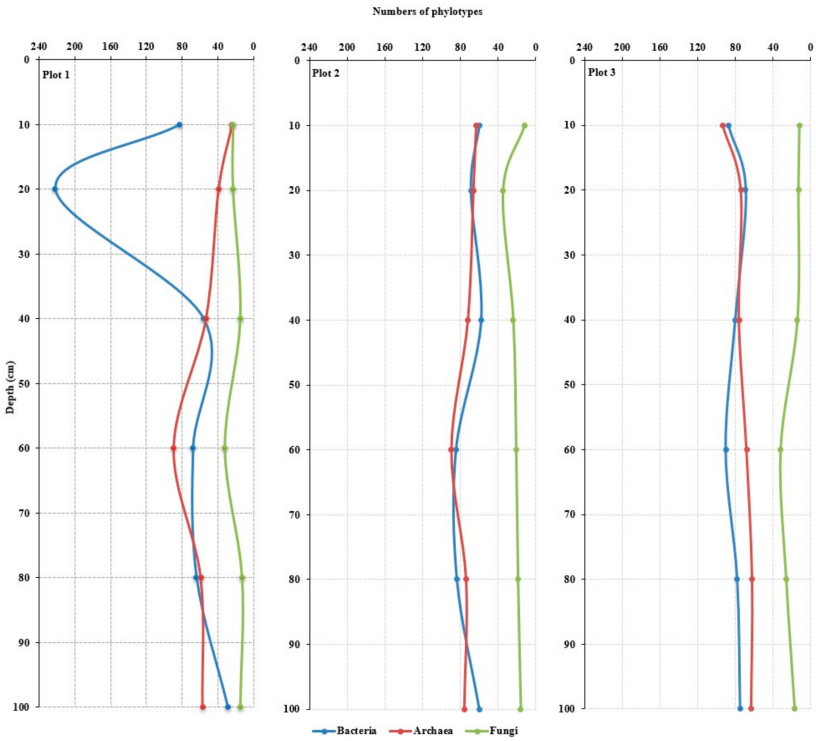

Figure 4. Vertical changes in numbers of bacteria, archaea, and fungi phylotypes detected along the investigated soil depth in each plot (bacteria as blue dots, archaea as red squares, and fungi as green triangles). The number of phylotypes corresponds to the number of bands on the T-RFLP profiles.

Numbers of bacteria and archaea phylotypes decreased with increasing soil depths in plots 1 and 2, while plot 3 showed the opposite trend. Particularly, those communities exhibited an increasing number of phylotypes at increasing soil depths similarly in the three plots. On the contrary, numbers of fungi phylotypes decreased. We obtained community groups using an arbitrary analysis of upper-active (0–20 cm), intermediate (20–60 cm), and deeper (60–100 cm) soil layers (Figure 4). A Bray–Curtis cluster analysis on the microbial community groups revealed that the archaea composition was similar in the upper and deeper layers in plot 1 and in plot 2, while in plot 3, all groups except that of the surface layer showed similar characteristics (Figure 5). In plot 1, the superficial and the intermediate layers grouped together were different from the deeper layer, while in plot 2 a similarity among the superficial and the deepest layers was observed. Plot 3 displayed a clear shift in the community along the soil depth gradient (Figure 5). For fungi, plot 1 displayed a complex similarity trend. The deeper layer grouped with the intermediate layer showed a different pattern with respect to 0–10 cm and 40–60 cm, highlighting the fungi community heterogeneity within the soil layers, and the homogeneity throughout the layers. Plot 2 and plot 3 showed similar fungal composition patterns, i.e., heterogeneity within groups, with a shift in patterns along the depth gradient.

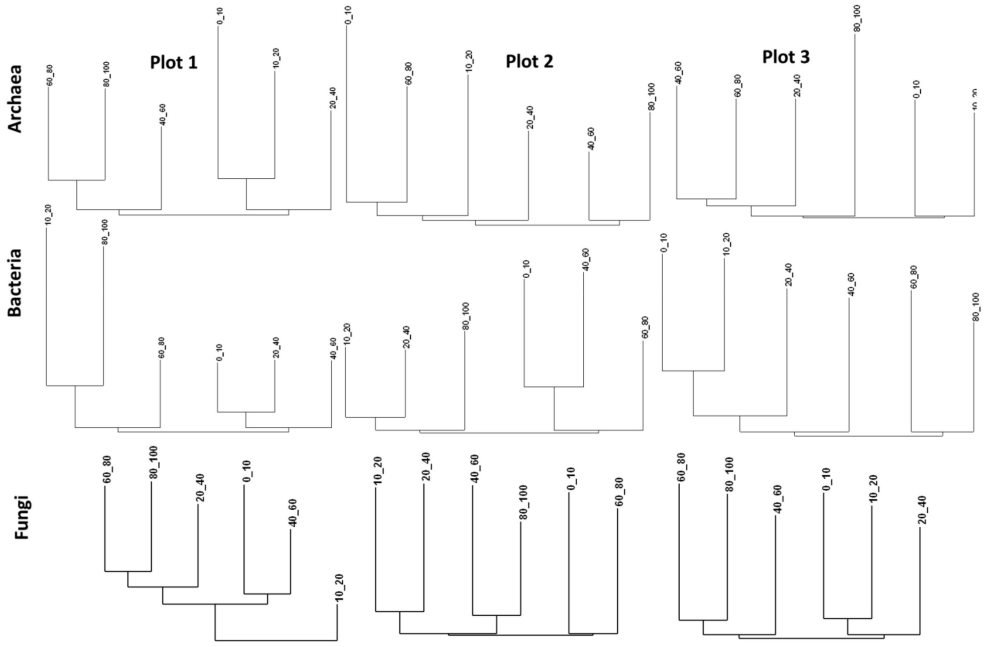

Figure 5. Dendrograms show similarity of T-RFLP profiles using Bray–Curtis hierarchical cluster analysis along the investigated soil depth in each plot.

The diversity of the bacteria community of plot 1 decreased along the depth gradient, except at 10–20 cm (Figure 6). The opposite was observed in plots 2 and 3, where the intermediate and deeper layers supported a significantly higher ($p < 0.05$) diversity of bacteria (Figure 6).

As regards the archaea diversity, plot 1 displayed an opposite trend along the depth gradient compared with plots 2 and 3. The fungi community's diversity showed a similar trend in plots 1 and 2 along the depth profile, while plot 3 showed a more stable value in the three layers (Figure 6).

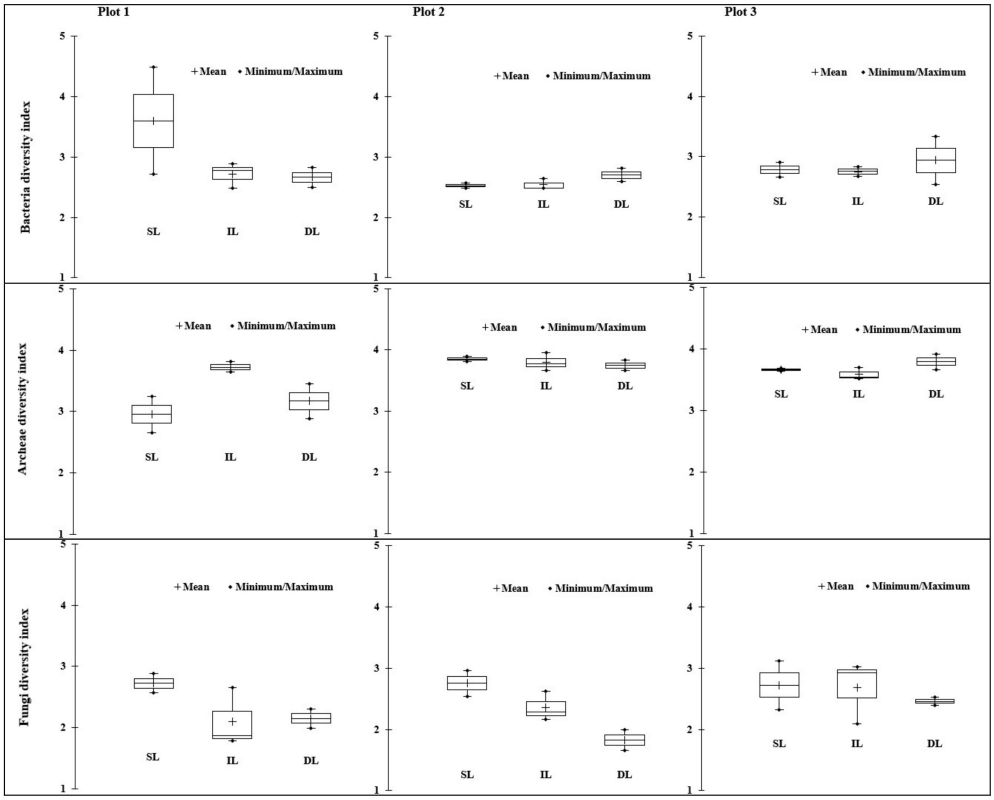

Figure 6. Boxplots of diversity index (Shannon index; H'). Three different soil layers (i.e., SL, superficial layer; IL, intermediate layer; and DL, deeper layer) were discriminated according to an arbitrary analysis of soil profile. Diversity was calculated from the number and the relative peak area of bands on the T-RFLP profiles.

3.4. Main Patterns of Chemical, Physical, and Microbiological Parameters as Affected by Soil Depth in Three Different Plots

The PCA was performed with data from soil and soil microbial community profiles and abundance, summarizing the correlations between all the parameters measured at 0–20 cm (Figure 7a). The first two discriminating components accounted for 45.48% and 32.20% of the total variability. In the case of parameters measured at 0–20 cm, three different latent patterns were identified, including (i) fungi abundance and diversity, soil CO_2 emissions, C/N ratio, and soil temperature; (ii) archaea and bacteria abundance, pH, soil respiration rate (*Rs*), and SOC; and (iii) soil chemical parameters linked to nitrogen. These results indicated a specificity of C/N ratio, fungi abundance, and soil CO_2 emissions in terms of soil parameters' variability at 0–20 cm. In plot 1 (Figure 7b), PC 1 (59.17%) and PC 2 (16.87%) explained 75% of the total variability of the data, displaying a different variability of soil properties and microbial community diversity and abundance in comparison with plots 2 and 3 (Figure 7c,d). In plot 2, PC 1 (48.70%) and PC 2 (32.52%) accounted for 81% of the variance. These results indicate a specificity of SOC and TN concentrations and the abundance of bacteria community in terms of soil parameters variability at the shallowest and deepest layers. In plot 3, PC 1 (60.10%) and PC 2 (22.74%) explained 83% of the total variability of the data, displaying a different variability of soil properties and microbial community diversity and abundance (Figure 7d). We used Spearman's rank correlation to examine how soil properties and microbial diversity and processes influenced the soil CO_2 emissions in the three plots investigated at 0–20 cm (Table S1). Soil temperature was positively correlated with the soil CO_2 emissions, measured with the portable chamber and *Nitr* rate, and was negatively correlated with fungi abundance (Fungi). Soil CO_2 emissions were positively correlated with the *Nitr* rate, while soil pH was positively correlated with soil CO_2 flux, *Rs*, *Nitr*, and archaea H', and was negatively correlated with fungi H'.

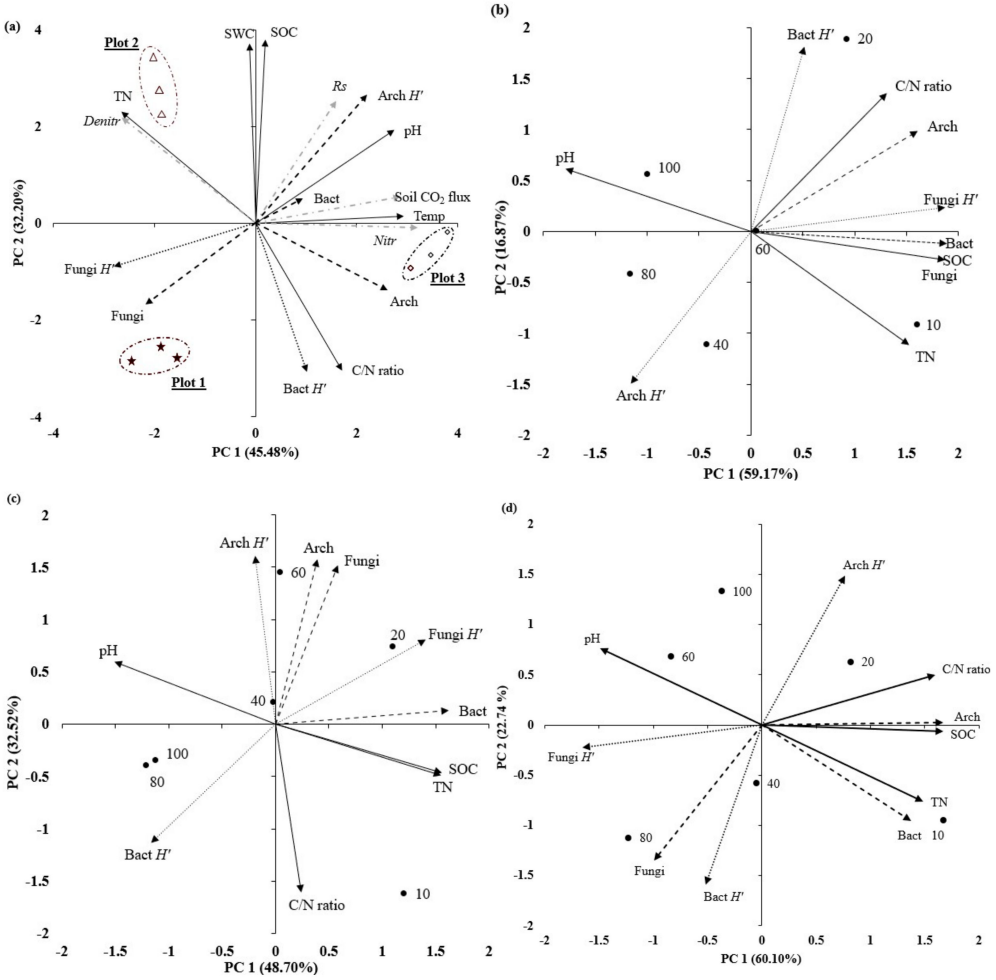

Figure 7. Principal component analysis (PCA) biplot was based on soil chemical and physical parameters (pH; SOC: soil organic carbon concentration; TN: total nitrogen concentration; C/N ratio; SWC: soil water content; Soil Temp: soil temperature), microbial processes *(Rs*: soil respiration; *Denitr*: denitrification rate; *Nitr*: gross nitrification rate), soil CO_2 emissions (measured using survey soil respiration chamber), microbial abundance (*Arch*: Archaea abundance; *Bact*: bacteria abundance; *Fungi*: fungi abundance) and Shannon index (Arch *H*′: Archaea Shannon index; Bact *H*′: Bacteria Shannon index; Fungi *H*′: Fungi Shannon index). All such parameters were used as variables, while replicate plots were used as observations in the 0–20 cm soil depth. Soil chemical and physical variables are shown by black continuous arrows, microbial processes and soil CO_2 emissions are shown by grey heavy dotted arrows, microbial *H*′ is shown by black heavy dotted arrows, and microbial abundance is shown by light dotted arrows. Observations are represented by black stars (plot 1), white triangles (plot 2), and white squares (plot 3). PC 1 and PC 2 axes together accounted for 77.78% of the variability and were significant ($p < 0.05$) (**a**). PCA biplot was based on soil chemical parameters, microbial abundance, and *H*′, which were used as variables, while soil depths were considered as observations. Observations (10: 0–10 cm, 20:10–20 cm, 40: 20–40 cm, 60: 40–60 cm, 80: 60–80 cm, 100: 80–100 cm) are represented by black circles. In plot 1, the PC 1 and PC 2 axes together accounted for 76.04% of the variability and were significant ($p < 0.05$) (**b**); in plot 2, the PC 1 and PC 2 axes together accounted for 81.22% of the variability and were significant ($p < 0.05$) (**c**); in plot 3, the PC 1 and PC 2 axes together accounted for 82.84% of the variability and were significant ($p < 0.05$) (**d**).

4. Discussion

So far, numerous studies have investigated ecosystem CO_2 emissions and changes in soil chemical properties and microbial processes and structure, but there is a lack of knowledge regarding the microbial spatial variability at different soil depths and the

influence of the microbial community in regulating C biogeochemical cycle. In recent years, Flores-Rentería et al. [50] found that CO_2 emissions occurring in soils from biological processes (i.e., autotrophic and heterotrophic components) were mainly affected by soil environmental abiotic factors such as moisture and temperature. These results confirm our findings that highlight significant spatial and temporal variability in terms of CO_2 emissions and microbial abundance, diversity, and processes within a peri-urban Mediterranean holm oak forest. Therefore, the increasing fragmentation of forests may profoundly influence the functioning of the plant–soil–microbial system, with important effects on CO_2 emissions and nutrient cycling at the ecosystem level.

At the ecosystem level, environmental control over soil CO_2 emissions is widely recognized [51]. Nevertheless, we observed that although soil temperature and moisture are interacting [52], few localized measurements made at a single point do not represent the overall ecosystem conditions [21], neither do they sufficiently explain the soil moisture's effect on soil CO_2 emissions. Thus, measurements at a larger scale with a much higher abundance of sampling plots would be required to better identify the effect of soil moisture on soil CO_2 emissions. In this context, Curiel Yuste et al. [53] found that the CO_2 emissions and soil microbial diversity in Mediterranean holm oak forests are influenced by abiotic and biotic factors such as water availability, forest fragmentation, and taxonomic diversity of soil bacteria communities.

Similarly, the highest soil CO_2 emissions occurred in plot 3 of our field study. This may be explained by biotic factors such as diversity in the abundance and composition of the soil microbial community within the plots [51]. Therefore, soil CO_2 emissions may be driven both by differences in autotrophic respiration components, linked to the complex effects of trees on soil properties (e.g., ectomycorrhizas associated with *Q. ilex*) and by heterotrophic respiration component, linked to the diversity and structure of soil microbial communities [54,55]. The great microbial diversity, mostly due to bacteria, suggests that the overall ecosystem contribution to soil CO_2 emissions is the result of highly heterogeneous patches of Soil In this context, Ruiz Gómez et al. [56] found that changes in the structure and functionality of the soil microbiome may influence tree health status. Particularly, they found that the decline of holm oak is related to the increase in the relative abundance of soil microbial functional genes associated with denitrification and phosphorus mineralization, affecting soil nutrient availability and tree health.

These results of the *Rs* rate measured using BaPS analysis were consistent with previous works showing that heterogeneity in soil chemical and physical properties affect the microbial processes and spatial distribution [57,58].

In the present study, despite the highest densities of microorganisms occurring in the surface 25 cm, the microbial groups residing in the deeper layers were described as assembling into a highly specialized community [59–61]. Thus, in our soil, different microbial communities may reside in the deepest soil layers in response to different soil physico-chemical parameters. These results are consistent with those reported by other authors. In a study conducted in 2011, Šrursová et al. [62] found that in forest soils the pH showed a more pronounced impact on the soil's microbial community diversity than in other soils. In 2014, Alele et al. [18] examined how the conversion of a natural forest directly influences the composition of soil bacteria and fungi microbial communities, also highlighting the changes occurring in other soil parameters, such as pH and SOC, which were also associated with spatial distribution linked with the composition of some soil microbial communities. Thus, soil pH values in Castelporziano may have driven changes in the relative abundance of some bacteria and archaea classes. This supports the hypothesis that fungi promote bacteria growth by enhancing the decomposition of soil organic matter [63], and by providing substrates or exudates that enhance the increase of bacteria from the superficial to the intermediate layer. The different composition of the microbial communities in the plots, as well as the heterogeneity observed in the emissions in laboratory conditions though the BaPS analysis, reflects that functionalities are differently distributed in soil, as shown by the *Nitr* rate and the *Denitr* rate [64]. In the present study,

T-RFLP patterns showed that quantitative differences among bacteria, archaea, and fungi communities exist up to a depth of 100 cm in forest soils. The positive correlation between archaea abundance and SOC indicates that SOC provides a crucial fraction of C to sustain the archaea communities. These differences might be due to microbial physiologies and sensitivities to environmental fluctuations, which represent a strong ecological filter [65]. The high numbers of bacteria and archaea bands, together with the specific trend observed, suggests the predominance of a specific set of taxonomic groups. Moreover, different ecological niches exist in space along both horizontal and vertical axes according to soil parameters. It is likely that one of the key drivers responsible for the observed variability may be the nutrient resource availability being patchily distributed [60]. Soil microbes and their processes are inextricably linked to above-ground communities. Therefore, soil surface litter can be a key co-factor affecting the vertical and horizontal microbial differentiation. Multivariate and cluster analysis confirmed our hypothesis, showing correlations between soil parameters and microbial communities' composition, as well as microbial assemblages and diversity in vertical space across the three plots investigated.

5. Conclusions

Our research on the spatial variability of the soil CO_2 emissions combined with soil physico-chemical properties and microbial processes and diversity showed that in the homogenous and photosynthetically active peri-urban holm oak Mediterranean forest of Castelporziano, the spatial variability of CO_2 emissions is strictly linked to the highly heterogeneous soil microbial assemblage and diversity among plots and soil depths. Bacteria dominated the microbial community and showed higher variability than fungi and archaea at all depths examined. Soil microbial processes were strongly correlated with the soil properties, particularly ther pH, soil water content, and SOC. The spatial heterogeneity of soil CO_2 emissions was associated with heterogeneity in the soil microbial community distribution. Considering that Mediterranean forest ecosystems are among the most threatened forest ecosystems by climate changes, microbial dynamics in response to changes in environmental conditions may largely affect the future carbon cycle.

In this study, bacteria showed higher variability than fungi and archaea at all depths examined. Such an insight showed the clear ecological and environmental implications of soil in the overall sustainability of peri-urban forest system. Our findings contribute to understanding the transformation processes of C in Mediterranean forest soils.

However, further studies on Mediterranean forests should focus on clarifying and accurately quantifying the relationship between soil CO_2 emissions and environmental drivers at plot and watershed scales. Innovative tools based on remote sensing and modelling integrated approach are needed to improve our understanding of CO_2 dynamics from heterogeneous soils.

Supplementary Materials: The following supporting information associated with this article can be downloaded at: https://www.mdpi.com/article/10.3390/f15112018/s1, Table S1: Spearman correlation coefficient matrix (similarity within the interval [−1; +1]) of soil physical and chemical parameters (SWC: soil water content; Soil Temp: soil temperature; pH: pH in water; SOC: soil organic carbon; TN: total nitrogen; C/N ratio), soil CO_2 flux (i.e., soil CO_2 emissions), microbial processes (*Rs*: soil respiration; *Nitr*: gross nitrification rate; *Denitr*: denitrification rate), and microbial abundance (Arch: Archaea abundance; Bact: Bacteria abundance; Fungi: Fungi abundance) and Shannon index (Arch H': Archaea Shannon index; Bact H': Bacteria Shannon index; Fungi H': Fungi Shannon index) expressed as mean of three plots at 0–20 cm soil depth. Significant correlations ($p < 0.05$; two-tailed test) are in bold print.

Author Contributions: Conceptualization, C.D.B., L.C. and R.F. (Roberta Farina); methodology, C.D.B., L.C., M.M. and R.F. (Roberta Farina); formal analysis, C.D.B., L.C., M.M., R.F. (Roberta Farina) and R.F. (Rosa Francaviglia); investigation, C.D.B. and R.F. (Roberta Farina); data curation, C.D.B., L.C. and R.F. (Roberta Farina); writing—original draft preparation, C.D.B. and L.C.; writing—review and editing, C.D.B., L.C., M.M., R.F. (Roberta Farina) and R.F. (Rosa Francaviglia). All authors have read and agreed to the published version of the manuscript.

Funding: This research received no external funding.

Data Availability Statement: Data are available upon request to the authors.

Acknowledgments: The authors wish to thank the Scientific Commission of Castelporziano for technical and logistic support, allowing the execution of these studies and the publication of the data; and the Multi-disciplinary Center for the Study of Coastal Mediterranean Ecosystems. We also thank the General Secretariat of the Presidency of Italian Republic for financing the CASTEL3 project, and the Directorate of Castelporziano Estate. We also wish to thank Silvano Fares for his valuable help in setting up the case study in the Castelporziano Estate. Special thanks are dedicated to Flavia Savi, Valerio Moretti, Tiziano Sorgi, and Filippo Ilardi for their technical support in field sampling and data collection.

Conflicts of Interest: The authors declare no conflicts of interest.

References

1. Cook, B.I.; Anchukaitis, K.J.; Touchan, R.; Meko, D.M.; Cook, E.R. Spatiotemporal drought variability in the Mediterranean over the last 900 years. *J. Geophys. Res. Atmos.* **2016**, *121*, 2060–2074. [CrossRef] [PubMed]
2. Fares, S.; Alivernini, A.; Conte, A.; Maggi, F. Ozone and particle fluxes in a Mediterranean forest predicted by the AIRTREE model. *Sci. Total Environ.* **2019**, *682*, 494–504. [CrossRef] [PubMed]
3. Bou Dagher-Kharrat, M.; de Arano, I.M.; Zeki-Bašken, E.; Feder, S.; Adams, S.; Briers, S.; Fady, B.; Lefèvre, F.; Górriz-Mifsud, E.; Mauri, E.; et al. *Mediterranean Forest Research Agenda 2030*; European Forest Institute: Barcelona, Spain, 2022; ISBN 978-952-7426-30-2/978-952-7426-31-9. [CrossRef]
4. Escobedo, F.; Kroeger, T.; Wagner, J. Urban forests and pollution mitigation: Analyzing ecosystem services and disservices. *Environ. Pollut.* **2011**, *159*, 2078–2087. [CrossRef] [PubMed]
5. Bussotti, F.; Pollastrini, M.; Holland, V.; Brüggemann, W. Functional traits and adaptive capacity of European forests to climate change. *Environ. Exp. Bot.* **2015**, *111*, 91–113. [CrossRef]
6. Pizzeghello, D.; Francioso, O.; Concheri, G.; Muscolo, A.; Nardi, S. Land Use Affects the Soil C Sequestration in Alpine Environment NE Italy. *Forests* **2017**, *8*, 197. [CrossRef]
7. Dobbs, C.; Escobedo, F.J.; Zipperer, W.C. A framework for developing urban forest ecosystem services and goods indicators. *Landsc. Urban Plan.* **2011**, *99*, 196–206. [CrossRef]
8. Maier, M.; Paulus, S.; Nicolai, C.; Stutz, K.P.; Nauer, P.A. Drivers of Plot-Scale Variability of CH_4 Consumption in a Well-Aerated Pine Forest Soil *Forests* **2017**, *8*, 193. [CrossRef]
9. Xu, W.; Cai, Y.P.; Yang, Z.F.; Yin, X.A.; Tan, Q. Microbial nitrification denitrification and respiration in the leached cinnamon soil of the upper basin of Miyun Reservoir. *Sci. Rep.* **2017**, *7*, 42032. [CrossRef]
10. Vesterdal, L.; Clarke, N.; Sigurdsson, B.D.; Gundersen, P. Do tree species influence soil carbon stocks in temperate and boreal forests? *For. Ecol. Manag.* **2013**, *309*, 4–18. [CrossRef]
11. Mou, R.; Jian, Y.; Zhou, D.; Li, J.; Yan, Y.; Tan, B.; Xu, Z.; Cui, X.; Li, H.; Zhang, L.; et al. Divergent responses of woody plant leaf and root non-structural carbohydrates to nitrogen addition in China: Seasonal variations and ecological implications. *Sci. Total Environ.* **2024**, *950*, 175425. [CrossRef]
12. Shvaleva, A.; Costa e Silva, F.; Costa, J.M.; Correia, A.; Anderson, M.; Lobo-do-Vale, R.; Fangueiro, D.; Bicho, C.; Pereira, J.S.; Chaves, M.M.; et al. Comparison of methane nitrous oxide fluxes and CO_2 respiration rates from a Mediterranean cork oak ecosystem and improved pasture. *Plant Soil* **2014**, *374*, 883–898. [CrossRef]
13. Tian, J.; McCormack, L.; Wang, J.; Guo, D.; Wang, Q.; Zhang, X.; Yu, G.; Blagodatskaya, E.; Kuzyakov, Y. Linkages between the soil organic matter fractions and the microbial metabolic functional diversity within a broad-leaved Korean pine forest. *E. J. Soil Biol.* **2015**, *66*, 57–64. [CrossRef]
14. Yachi, S.; Loreau, M. Biodiversity and ecosystem productivity in a fluctuating environment: The insurance hypothesis. *Proc. Natl. Acad. Sci. USA* **1999**, *96*, 1463–1468. [CrossRef] [PubMed]
15. Ettema, C.H.; Wardle, D.A. Spatial soil ecology. *Trends Ecol. Evol.* **2002**, *17*, 177–183. [CrossRef]
16. Coleman, D.C.; Whitman, W.B. Linking species richness biodiversity and ecosystem function in soil systems. *Pedobiologia* **2005**, *49*, 479–497. [CrossRef]
17. Levine, U.Y.; Teal, T.K.; Robertson, G.P.; Schmidt, T.M. Agriculture's impact on microbial diversity and associated fluxes of carbon dioxide and methane. *ISME J.* **2011**, *5*, 1683–1691. [CrossRef]
18. Alele, P.O.; Sheif, D.; Surget-Groba, Y.; Lingling, S.; Cannon, C.H. How does conversion of natural tropical rainforest ecosystems affect soil bacterial and fungal communities in the Nile River watershed of Uganda? *PLoS ONE* **2014**, *9*, e104818. [CrossRef]
19. Soil Survey Staff. *Soil Taxonomy: A Basic System of Soil Classification for Making and Interpreting Soil Surveys*; USDA-SCS Agric. Handb. 436. U.S. Gov. Print: Washington, DC, USA, 1975.
20. IUSS Working Group WRB. *World Reference Base for Soil Resources 2006*; World Soil Resources Reports No. 103; FAO: Rome, Italy, 2006.
21. Savi, F.; Di Bene, C.; Canfora, L.; Mondini, C.; Fares, S. Environmental and biological controls on CH_4 exchange over an evergreen Mediterranean forest. *Agric. For. Meteorol.* **2016**, *226–227*, 67–79. [CrossRef]

22. Fusaro, L.; Mereu, S.; Salvatori, E.; Agliari, E.; Fares, S.; Manes, F. Modelling ozone uptake by urban and peri-urban forest: A case study in the Metropolitan City of Rome. *Environ. Sci. Pollut. Res.* **2018**, *25*, 8190–8205. [CrossRef]
23. Napoli, R.; Paolanti, M.; Di Ferdinando, S. *Atlante dei Suoli del Lazio*; ARSIAL Regione Lazio; Società Elaborazioni Cartografiche (S EL. CA. s.r.l.): Firenze, Italy, 2019; ISBN 978-88-90484I-2-4.
24. Luo, Y.; Zhou, X. *Soil Respiration and the Environment*; Elsevier: London, UK, 2006; p. 316.
25. Kutsch, W.L.; Bahn, M.; Heinemeyer, A. *Soil Carbon Dynamics: An Integrated Methodology*; Cambridge University Press: New York, NY, USA, 2009; p. 286.
26. Heinemeyer, A.; Di Bene, C.; Lloyd, A.R.; Tortorella, D.; Baxter, R.; Huntley, B.; Gelsomino, A.; Ineson, P. Soil respiration: Implications of the plant-soil continuum and respiration chamber collar-insertion depth on measurement and modelling of soil CO_2 efflux rates in three ecosystems. *Eur. J. Soil Sci.* **2011**, *62*, 82–94. [CrossRef]
27. Pumpanen, J.; Kolari, P.; Ilvesniemi, H.; Minkkinen, K.; Vesala, T.; Niinistö, S. Comparison of different chamber techniques for measuring soil CO_2 efflux. *Agr. Forest Meteorol.* **2004**, *123*, 159–176. [CrossRef]
28. Asensio, D.; Peñuelas, J.; Llusià, J.; Ogaya, R.; Filella, I. Interannual and interseasonal soil CO_2 efflux and VOC exchange rates in a Mediterranean holm oak forest in response to experimental drought. *Soil Biol Biochem.* **2007**, *39*, 2471–2484. [CrossRef]
29. Rey, A.; Pegoraro, E.; Tedeschi, V.; de Parri, I.; Jarvis, P.G.; Valentini, R. Annual variation in soil respiration and its components in a coppice oak forest in Central Italy. *Global Chang. Biol.* **2002**, *8*, 851–866. [CrossRef]
30. FAO. *Guidelines for Soil Description*, 4th ed.; Food and Agriculture Organisation of the United States: Rome, Italy, 2006; p. 109. Available online: http://www.fao.org/3/a-a0541e.pdf (accessed on 27 August 2024).
31. Pritchett, W.L.; Fisher, R.F. *Properties and Management of Forest Soils*, 2nd ed.; Wiley: New York, NY, USA, 1982; p. 494.
32. Pinzari, F.; Trinchera, A.; Benedetti, A.; Sequi, P. Use of biochemical indices in the mediterranean environment: Comparison among soils under different forest vegetation. *J. Microbiol. Meth* **1999**, *36*, 21–28. [CrossRef]
33. Mocali, S.; Paffetti, D.; Emiliani, G.; Benedetti, A.; Fani, R. Diversity of heterotrophic aerobic cultivable microbial communities of soils treated with fumigants and dynamics of metabolic microbial and mineralization quotients. *Biol. Fert. Soils* **2008**, *44*, 557–569. [CrossRef]
34. USDA-NRCS. *Soil Survey Laboratory Methods Manual*, Soil Survey Inv. Rep. N. 42 Version 3.0; USDA: Washington, DC, USA, 1996.
35. McLean, E.O. Soil pH and lime requirement. In *Methods of Soil Analysis Part 2 Chemical and Microbiological Properties*, 2nd ed.; Page, A.L., Miller, R.H., Keeney, D.R., Eds.; Agronomy Monograph 9 American Society of Agronomy: Madison, WI, USA, 1982; pp. 199–224.
36. Munz, H.; Ingwersen, J.; Streck, T. On-site sensor calibration procedure for quality assurance of Barometric Process Separation (BaPS) measurements. *Sensors* **2023**, *23*, 4615. [CrossRef]
37. Creamer, R.E.; Schulte, R.P.O.; Stone, D.; Gal, A.; Krogh, P.H.; Lo Papa, G.; Murray, P.J.; Pérès, G.; Foerster, B.; Rutgers, M.; et al. Measuring basal soil respiration across Europe: Do incubation temperature and incubation period matter? *Ecol. Indicator* **2014**, *36*, 409–418. [CrossRef]
38. Lu, X.; Yan, Y.; Fan, J.; Wang, X. Gross Nitrification and Denitrification in Alpine Grassland Ecosystems on the Tibetan Plateau. *Arct. Antarct. Alp. Res.* **2012**, *44*, 188–196. [CrossRef]
39. Brunori, E.; Farina, R.; Blasi, R. Sustainable viticulture: The carbon-sink function of the vineyard agro-ecosystem. *Agr. Ecosyst. Environ.* **2016**, *223*, 10–21. [CrossRef]
40. Canfora, L.; Lo Papa, G.; Vittori Antisari, L.; Dazzi, C.; Benedetti, A. Spatial microbial community structure and biodiversity analysis in "extreme" hypersaline soils of a semiarid Mediterranean area. *Appl. Soil Ecol.* **2015**, *93*, 120–129. [CrossRef]
41. Liu, W.T.; Marsh, T.L.; Cheng, H.; Forney, L.J. Characterization of microbial diversity by determining terminal restriction fragment length polymorphisms of genes encoding 16 S rRNA. *App Environ. Microb.* **1997**, *63*, 4516–4522. [CrossRef] [PubMed]
42. Gardes, M.; Bruns, T.D. ITS primers with enhanced specificity for Basidiomycetes—Application to the identification of mycorrhizae and rusts. *Mol. Ecol.* **1993**, *2*, 113–118. [CrossRef] [PubMed]
43. Hammer, Ø.; Harper, D.A.T.; Ryan, P.D. PAST: Paleontological Statistic software package for education and data analysis. *Paleontol. Eletron.* **2001**, *4*, 1–9. Available online: http://palaeo-electronica.org/2001_1/past/past.pdf (accessed on 27 August 2024).
44. Hill, T.C.J.; Walsh, K.A.; Harris, J.A.; Moffett, B.F. Using ecological diversity measures with bacterial communities. *FEMS Microbiol. Ecol.* **2003**, *43*, 1–11. [CrossRef] [PubMed]
45. Nadkarni, M.A.; Martin, F.E.; Jacques, N.A.; Hunter, N. Determination of bacterial load by real-time PCR using a broad-range (universal) probe and primers set. *Microbiology* **2002**, *148*, 257–266. [CrossRef]
46. Ochsenreiter, T.; Selezi, D.; Quaiser, A.; Bonch-Osmolovskaya, L.; Schleper, C. Diversity and abundance of Crenarchaeota in terrestrial habitats studied by 16S RNA surveys and real time PCR. *Environ. Microbiol.* **2003**, *5*, 787–797. [CrossRef]
47. Vilgalys, R.; Hopple, J.S.; Hibbett, D.S. Phylogenetic implications of generic concepts in fungal taxonomy: The impact of molecular systematic studies. *Mycol. Res.* **1994**, *6*, 73–91. [CrossRef]
48. Töwe, S.; Albert, A.; Kleineidam, K.; Brankatschk, R.; Dümig, A.; Welzl, G.; Munch, J.C.; Zeye, J.; Schloter, M. Abundance of microbes involved in nitrogen transformation in the rhizosphere of *Leucanthemopsis alpina* (L.) HEYWOOD grown in soils from different sites of the Damma glacier forefield. *Microb. Ecol.* **2010**, *60*, 762–770. [CrossRef]
49. Ramette, A. Multivariate analyses in microbial ecology. *FEMS Microb. Ecol.* **2007**, *62*, 142–160. [CrossRef]

50. Flores-Rentería, D.; Rincón, A.; Morán-López, T.; Hereş, A.M.; Pérez-Izquierdo, L.; Valladares, F.; Curiel Yuste, J. Habitat fragmentation is linked to cascading effects on soil functioning and CO_2 emissions in Mediterranean holm-oak-forests. *Peer J.* **2018**, *30*, e5857. [CrossRef]
51. Davidson, E.A.; Janssens, I.A. Temperature sensitivity of soil carbon decomposition and feedback to climate change. *Nature* **2006**, *440*, 165–173. [CrossRef]
52. Webster, K.L.; Creed, I.F.; Skowronski, M.D.; Kaheil, Y.H. Comparison of the performance of statistical models that predict soil respiration from forests. *Soil Sci. Am. J.* **2009**, *73*, 1157–1167. [CrossRef]
53. Curiel Yuste, J.; Fernandez-Gonzalez, A.J.; Fernandez-Lopez, M.; Ogaya, R.; Penuelas, J.; Lloret, F. Functional diversification within bacterial lineages promotes wide functional overlapping between taxonomic groups in a Mediterranean forest Soil *FEMS Microbiol. Ecol.* **2014**, *90*, 54–67. [CrossRef] [PubMed]
54. Haskl, E.; Zechmeister-Boltenstern, S.; Bodrossy, L.; Sessitsch, A. Comparison of diversities and compositions of bacterial populations inhabiting natural forest soils. *App. Environ. Microb.* **2004**, *70*, 5057–5065. [CrossRef]
55. Lejon, D.P.H.; Chaussod, R.; Ranger, J.; Ranjard, L. Microbial community structure and density under different tree species in an acid forest soil (Morvan France). *Microb. Ecol.* **2005**, *50*, 614–625. [CrossRef]
56. Ruiz Gómez, F.J.; Navarro-Cerrillo, R.M.; Pérez-de-Luque, A.; Oβwald, W.; Vannini, A.; Morales-Rodríguez, C. Assessment of functional and structural changes of soil fungal and oomycete communities in holm oak declined dehesas through metabarcoding analysis. *Sci. Rep.* **2019**, *9*, 5315. [CrossRef]
57. Hansel, C.M.; Fendorf, S.; Jardine, P.M.; Francis, C.A. Changes in bacterial and archaeal community structure and functional diversity along a geochemically variable soil profile. *Appl. Environ. Microb.* **2008**, *74*, 1620–1633. [CrossRef]
58. Siciliano, S.D.; Palmer, A.S.; Winsley, T.; Lamb, E.; Bissett, A.; Brown, M.V.; Van Dorst, J.; Mukan, J.; Ferrari, B.C.; Grogan, P.; et al. Soil fertility is associated with fungal and bacterial richness whereas pH is associated with community composition in polar soil microbial communities. *Soil Biol. Biochem.* **2014**, *78*, 10–20. [CrossRef]
59. Rousk, J.; Baath, E.; Brookes, P.C.; Lauver, C.L.; Lozupone, C.; Caporaso, J.G.; Knight, R.; Fierer, N. Soil bacterial and fungal communities across a pH gradient in an arable Soil *ISME J.* **2000**, *4*, 1340–1351. [CrossRef]
60. Nacke, H.; Thurmer, A.; Wollherr, A.; Will, C.; Hodac, L.; Herold, N.; Schoning, I.; Schrumpf, M.; Daniel, R. Pyrosequencing-based assessment of bacterial community structure along different management types in German forest and grassland soils. *PLoS ONE* **2003**, *6*, e17000. [CrossRef]
61. Lauber, C.L.; Hamady, M.; Knight, R.; Fierer, N. Pyrosequencing-based assessment of soil pH as a predictor of soil bacterial community structure at the continental scale. *App Environ. Microb.* **2009**, *75*, 5111–5120. [CrossRef] [PubMed]
62. Šrursová, M.; Baldrian, P. Effects of soil properties and management on the activity of soil organic matter transforming enzymes and the quantification of soil-bound and free activity. *Plant Soil* **2011**, *338*, 99–110. [CrossRef]
63. De Boer, W.; Folman, L.B.; Summerbell, R.C.; Boddy, L. Living in a fungal world: Impact of fungi on soil bacterial niche development. *FEMS Microb. Rev.* **2005**, *29*, 795–811. [CrossRef]
64. Hayatsu, M.; Tago, K.; Saito, M. Various players in the nitrogen cycle: Diversity and functions of the microorganisms involved in nitrification and denitrification. *Soil Sci. Plant Nutr.* **2008**, *54*, 33–45. [CrossRef]
65. Ho, A.; Di Lonardo, D.P.; Bodelier, P.L.E. Revisiting life strategy concepts in environmental microbial ecology. *FEMS Microbiol. Ecol.* **2017**, *93*, fix006. [CrossRef]